International Journal of Precision Engineering and Manufacturing
https://doi.org/10.1007/s12541-024-01091-8

Online ISSN 2005-4602
Print ISSN 2234-7593

REGULAR PAPER

Study on Scratching Process of Alumina Ceramic by Diamond Indenter under Compressive Pre-stress

Gaofeng Zhang[1] · Yu Liao[1,2] · Yang Deng[1] · Chang Liang[1] · Hang Xiao[1] · Tiejun Song[2] · Gang He[2]

Received: 21 February 2024 / Revised: 19 July 2024 / Accepted: 22 July 2024

Abstract

The high hardness and brittleness of engineering ceramics make it difficult to ensure surface quality during conventional grinding. Compressive pre-stress assisted machining, as a new processing technology, can effectively improve the surface/subsurface damage of engineering ceramics. In this study, compressive pre-stress assisted scratching experiment was conducted on 95% Al_2O_3 ceramics with diamond indenter under three pre-stresses of 0 MPa, 200 MPa and 400 MPa. The influence of compressive pre-stress on the scratch morphology of 95% Al_2O_3 ceramics, as well as the changes in scratch force and vibration signal during the wear of indenter were comprehensively analyzed. The experimental results show that when the compressive pre-stress increases to 400 MPa, the scratch depth is reduced by 5–15%, the width is reduced by 10–30%, and the depth of scratch subsurface damage is also reduced, avoiding the occurrence of obvious cracks. Wavelet decomposition of the collected vibration signals shows that as the increase of the compressive pre-stress, the fluctuation value of singulars in high-frequency signals gradually decreases, and the percentage of energy gradually increases. Combined with wavelet analysis and the surface wear morphology of indenter, it was found that although the large compressive pre-stress aggravates the tool wear, the surface machining quality of the material is also significantly improved.

Keywords Al_2O_3 ceramics · Compressive pre-stress · Diamond indenter · Surface characteristic · Wavelet decomposition

1 Introduction

Engineering ceramics are increasingly used in various industrial applications due to their excellent physical and chemical properties [1–3]. Owing to the high hardness and brittleness of ceramic materials, grinding has become their primary machining method [4, 5]. However, traditional grinding processes often result in processing defects in ceramics, such as pores and cracks [6–8]. In order to reduce these defects, the application of compressive pre-stress in the machining of engineering ceramics has garnered widespread attention.

Compressive pre-stress machining is a new machining technology, which can effectively reduce the surface/subsurface damage of engineering ceramics by applying appropriate compressive pre-stress to the workpiece. In the previous study, Chen et al. [9] applied a certain stress around the cylindrical glass ceramics and conducted compression experiments under quasi-static and dynamic conditions. The results showed that when the stress value was 230 MPa, compared with no stress, the fracture mechanism of the material tended to change from brittle fracture to plastic deformation. Head and Cline [10] conducted quasi-static triaxial compression experiments on a variety of polycrystalline ceramics after applying certain compressive pre-stress, and found that the materials showed a transition from brittle fracture to plastic deformation. Masahiko et al. [11–13] conducted a series of researches on single-particle scratching and two-dimensional cutting of hard and brittle materials such as glass, ceramics and monocrystalline silicon under high hydrostatic pressure. The experimental results showed that when the high hydrostatic pressure reached 400 MPa, it effectively reduced the damage of machined surface, restrained the expansion of radial crack, and improved the surface quality of machined workpiece. Qu et al. [14] and Yang et al. [15] studied the damage in the grinding process of unidirectional and 2.5D-C/SiCs ceramics and found that fiber pull-out and fiber exposure are the basic damage modes

✉ Gaofeng Zhang
zgfxu@xtu.edu.cn

[1] School of Mechanical and Electrical Engineering, Changsha University, Changsha 410022, China

[2] School of Mechanical Engineering and Mechanics, Xiangtan University, Xiangtan 411105, China

Published online: 12 August 2024

of unidirectional C/SiCs. Interface debonding, matrix cracking, fiber pull-out and fiber exposure are the main defects of 2.5D-C/SiCs, and become more serious with the increase of grinding depth. Tan et al. have also done a lot of work on the compressive pre-stress processing of SiC and Al_2O_3 ceramics [16–19]. Through the experimental research on the single-point diamond scratch and grinding under unidirectional and bidirectional compressive pre-stress of SiC and Al_2O_3 ceramics, it is concluded that with the increase of pre-stress, the pre-stress of sic and Al_2O_3 ceramics can be improved. The crack propagation length and depth of surface/subsurface of scratched and ground workpiece were reduced, the surface roughness value was reduced, and low damage machining of ceramic materials was achieved. But during grinding, the depth and width of the scratch groove decreased to a certain extent, while the normal and tangential forces increased to a certain extent. Du et al. [19] found the residual stress of ceramics was increased after grinding under compressive pre-stress. In the conventional processing of engineering ceramics, the tool wear mechanism under different materials and processing parameters has been widely studied, including the uneven organization of the tool and workpiece, the effect of mechanical and thermal stress, and the change of cutting force [20–26]. Overall, the current research on compressive pre-stress machining of ceramics mainly focuses on surface quality, cutting force and residual stress. However, there are currently few comprehensive studies on compressive pre-stress machining of 95% Al_2O_3 ceramics, including crack growth, tool wear, vibration signals and cutting force.

This paper carried out a single-point diamond indenter scratch processing test on 95% Al_2O_3 ceramics under compressive pre-stress of 0 MPa, 200 MPa and 400 MPa. The surface and subsurface topography characteristics of the ceramic after the scratch test and the relationship between the indenter wear and cutting force and vibration signal during the machining process were systematically studied. The influence of compressive pre-stress on surface morphology and tool wear was analyzed, and the relationship of compressive pre-stress on cutting force and vibration signal was investigated by wavelet analysis, which provided guidance and suggestions for optimizing ceramic machining.

2 Experiment

2.1 Experimental Materials

The workpieces were 95% Al_2O_3 ceramics with a size of 10 mm × 10 mm × 10 mm, and the physical properties are presented in Table 1. Prior to the scratch test, a high-precision surface grinding machine (MGK7120X60/1, Hangzhou Machine Tool) was used to perform semi-finishing and fine grinding on the workpiece, and the grinding feeds were 5 μm and 1 μm, respectively. After grinding, the sample surface was polished using diamond abrasive pastes with grain sizes of 6.5 μm, 2 μm, and 0.5 μm in sequence on a nano-polishing machine (Nanopoli-100, Wistates Precision Technology Co., LTD). Finally, the polished samples were ultrasonically cleaned for 30 min. The cleaned sample was observed under an ultra-depth-of-field microscope (VHX-2000, Keyence) and the microstructure of the sample is shown in Fig. 1.

2.2 Experimental Scheme

The scratch test was performed using a self-built experimental platform. The compressive pre-stress was applied to the workpiece fixture to achieve two-dimensional compressive pre-stress load on the workpiece, as shown in Fig. 2. The

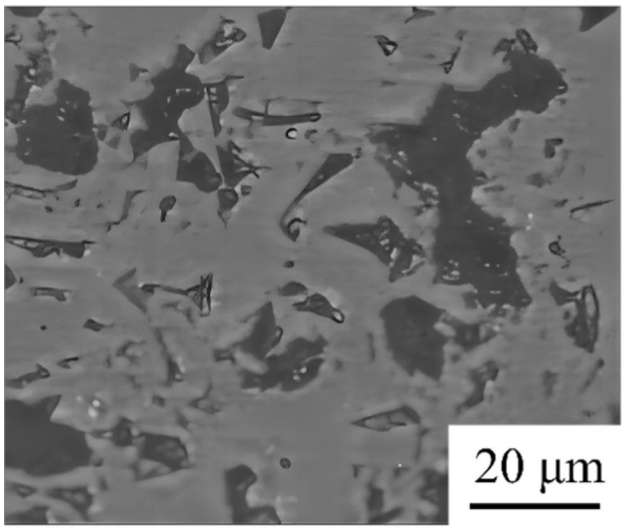

Fig. 1 Microstructure of 95% Al_2O_3 ceramic

Table 1 Physical properties of workpiece

Material	Density (g/cm$^{3)}$	Hardness (HRA)	Elastic modulus (GPa)	Poisson's ratio	Compressive strength (MPa)	Bending strength (MPa)	Fracture toughness (MPa m$^{1/2}$)
95% Al_2O_3	3.7	≥ 86	300	0.2	2500	≥ 300	3.5

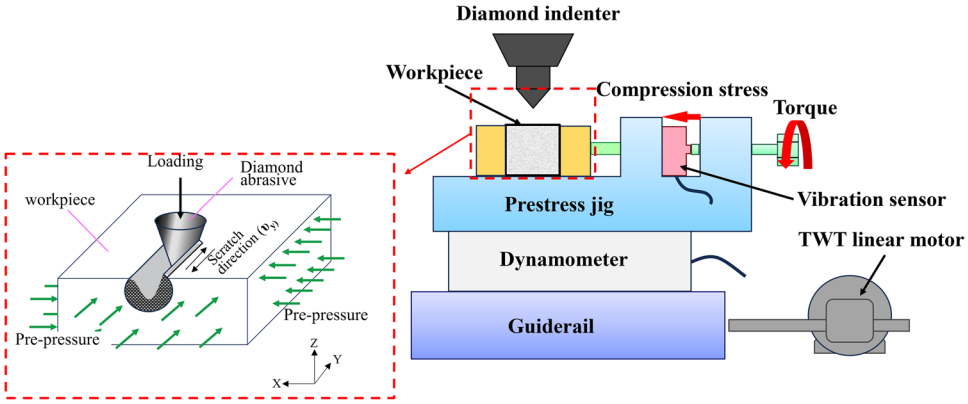

Fig. 2 Compressive pre-stress scratch experimental device schematic

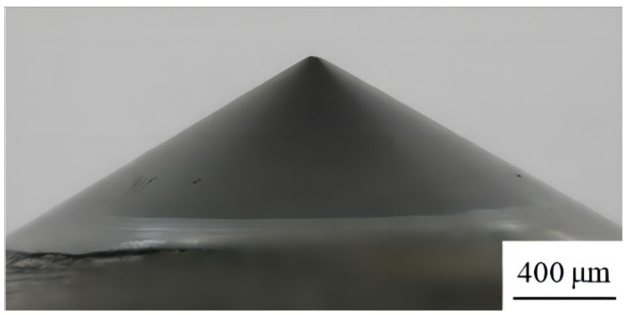

Fig. 3 Morphology of diamond indenter

Table 2 Experimental parameters

Parameter	Value
Speed (mm/min)	60
Depth (μm)	10
Scratch time (min)	150
Compressive pre-stress (MPa)	0, 200, 400

value of compressive pre-stress was controlled by the torsion plate hand. During the scratch experiment, the dynamometer (Kistler) and the pre-stressed fixture were installed together on the guide rail, and the guide rail was pushed by a linear motor (4RK25RGN-CM/4LB10-1, Taiwan T.W.T Motor Industry' Co., LTD) to drive the movement of the workpiece, thereby producing reciprocating scratches in which the dynamometer was used to measure online the changes in cutting force during the scratching process. The vibration generated during contact between the indenter and workpiece was monitored in real time using a vibration sensor (8793A, Kistler).

A diamond Rockwell indenter with a cone radius of 50 μm was used in the pre-pressure scratch experiment, as shown in Fig. 3. The parameters of the reciprocating scratch experiment are shown in Table 2, in which the compressive pre-stress test values are 0 MPa, 200 MPa, and 400 MPa. Each set of parameter experiments was repeated three times, and a fresh diamond indenter was used each time. The cutting force and vibration signals were collected every 10 min during the scratching process. After the scratch test, the workpiece was cleaned, and then the surface morphologies under different compressive pre-stresses were observed using an ultra-depth of field (VHX-2000, Keyence) and a scanning electron microscope (JSM-6360LV, Japan Electronics Co., LTD). In order to visually analyze the subsurface influence layer in the scratched area, the cross-section perpendicular to the scratch direction of the scratched workpiece was ground and polished.

3 Experimental

3.1 Surface and Subsurface Morphologies

The scratch surface morphologies of 95% Al_2O_3 ceramics under different compressive pre-stresses are shown in Fig. 4 (scratch time $\Delta t = 10$ min). With no compressive pre-stress, the width of the 95% Al_2O_3 ceramic scratch groove was the largest, the bottom of the groove was severely cracked, and many extended cracks appeared on both sides of the groove. With the increase of compressive pre-stress, the width of the groove gradually decreased, the degree of damage at the groove bottom decreased, and the peeling damage on the both sides of the groove decreased. This indicates that compressive pre-stress reduced the material removal rate but also reduced cracks in the ceramic material scratch process. The formation and propagation of cracks in ceramics during processing are caused mainly by external tensile stress [18]. As the compressive pre-stress increases, the compressive stress in the scratch area also increases correspondingly, followed by a decreased in the tensile stress. The reduction of tensile stress results in fewer cracks formed during material processing, and an increase in the internal strength of the material. The increase or decrease in material strength will affect the wear of the indenter to a certain extent.

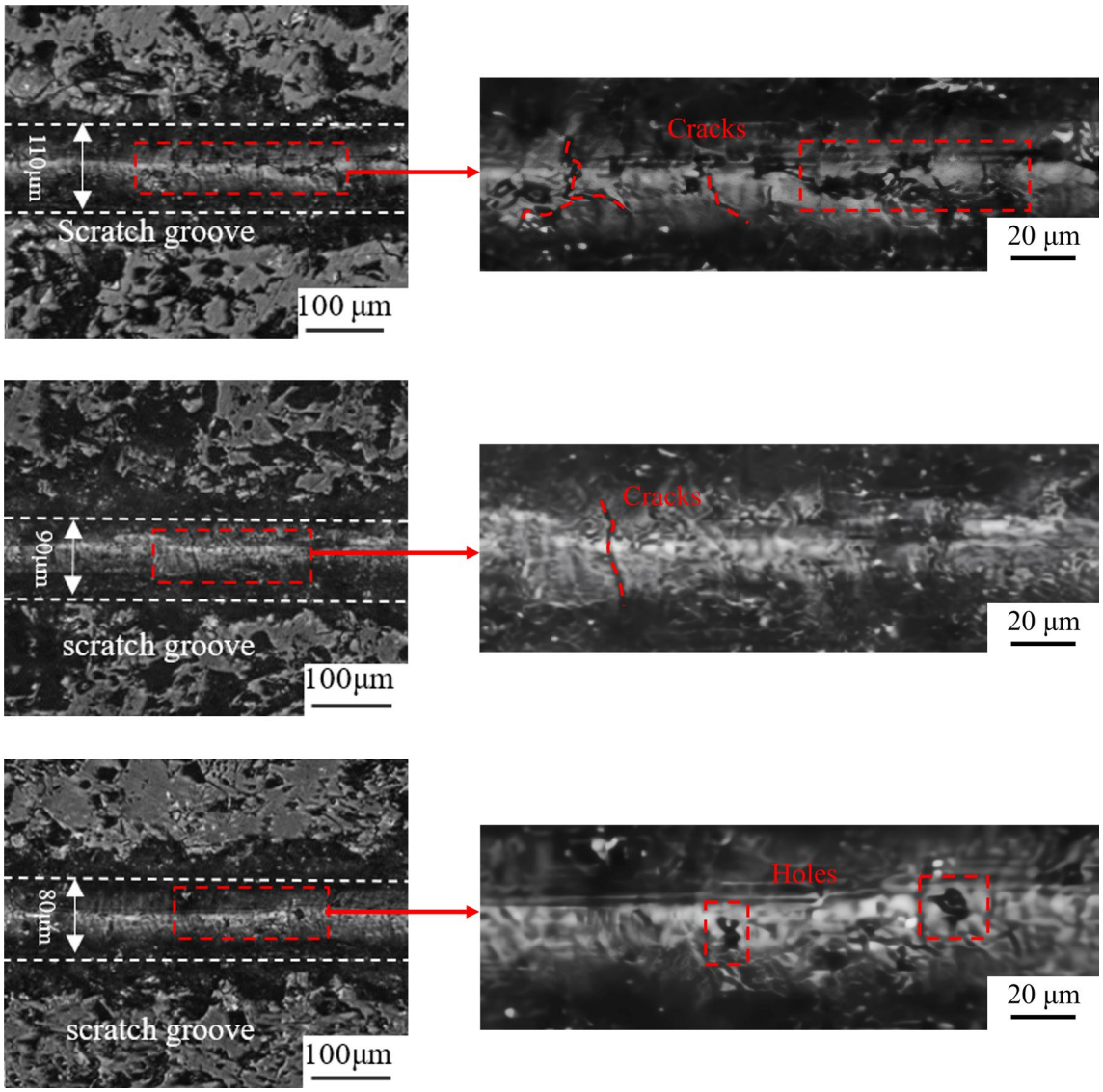

Fig. 4 Surface morphologies of scratched 95% Al_2O_3 ceramics under different compressive pre-stresses

The scratch groove profiles of 95% Al_2O_3 ceramics under different compressive pre-stresses are shown in Fig. 5. With no compressive pre-stress, due to the large contact and extrusion pressure between the indenter and the workpiece, the grains on both sides of the groove were broken or pulled out, eventually leading to the uneven cross-sectional profile of the groove. When the compressive pre-stress of 400 MPa was applied to the workpiece, there was a certain accumulation on both sides of the groove, and the entire groove profile curve was smooth, indicating that the compressive pre-stress inhibited the fracture of the groove edge and the spalling and pulling out of the grain, so there is no obvious damage. In addition, the depth and width of the groove decreased with the increase of the compressive pre-stress value, especially the width of the groove decreased obviously.

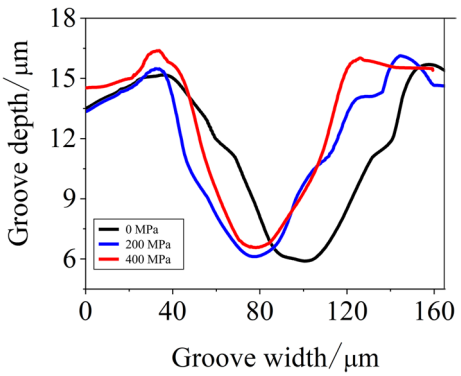

Fig. 5 Scratch groove profiles of 95% Al_2O_3 ceramic under different compressive pre-stress for 150 min

By using the section profile measurement function of the ultra-depth of field microscope, five points were randomly selected at any position of the scratch groove under the same scratch parameter, and the depth and width of the scratch groove were counted. The changes in groove depth and width of 95% Al_2O_3 ceramics under different scratch parameters are shown in Fig. 6. With the increase of compressive pre-stress, groove depth and width decrease to a certain extent. When the compressive pre-stress increases to 400 MPa, the groove depth and width decrease by 5–15% and 10–30% respectively. Due to the rigidity of the scratch system, deformation will occur after the continuous application of the compressive pre-stress. As the compressive pre-stress increases, the range of error bars for groove depth and width gradually decreases, which indicates that during the scratch process, the compressive pre-tress improves the flatness of groove bottom and edge, reduces the fracture and grain peeling at the groove bottom and edge, which reduces the scratch resistance at the groove depth and width.

In order to analyze the effect of compressive pre-stress on the range of scratch subsurface influence layer, the polished cross-sectional morphologies of the 95% Al_2O_3 ceramics under different pre-stresses were observed, as shown in Fig. 7. The depth of the broken layer of the scratch subsurface is reduced from 100 to 69 μm. With the increase of compressive pre-stress, the depth and area of the crushing layer of the scratch subsurface decrease, and the finish of the polished subsurface increases, but the width and depth of the scratch groove also decrease to a certain extent, indicating that the increase of compressive pre-stress can reduce the subsurface damage of engineering ceramics during the scratch processing.

In summary, with the increase of compressive pre-stress, the depth and width of the scratch groove are reduced to some extent, the bottom and edge quality of the scratch groove are improved.

3.2 Indenter Wear

As the wear of the indenter is not particularly great in the scratch test, to facilitate a subtle observation of indenter wear, a scanning electron microscope (JSM-6360LV) was used to observe the morphology, as shown in Figs. 8 and 9.

When scratch time $t_1 = 20$ min, there was no significant difference in the wear of the three indenter tips under different compressive pre-stresses. As shown in Fig. 8, the surface morphology of the indenter tip with pre-stress of 400 MPa had good integrity. There was no obvious wear and only slight scratch marks were observed at the tip of the indenter in contact with the workpiece. The morphologies of the indenter after the experiment are shown in Fig. 9. The edge of the tip under no compressive pre-stress exhibited some wear. With an increase in compressive pre-stress, the wear degree of the tip edge of the indenter increased. When the

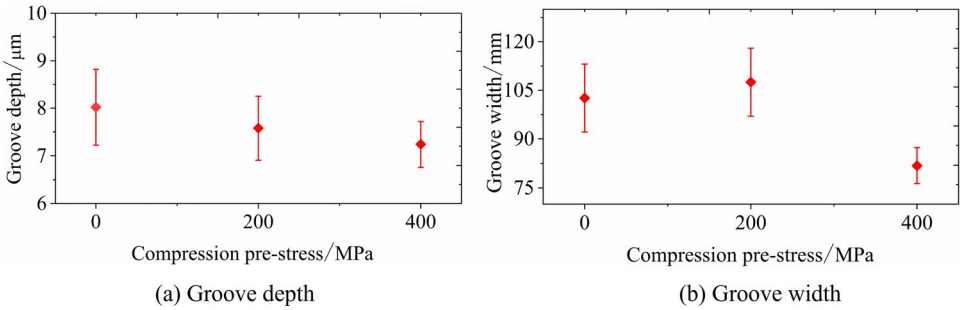

(a) Groove depth (b) Groove width

Fig. 6 95% Al_2O_3 ceramic scratches **a** groove depth and **b** groove width for 150 min

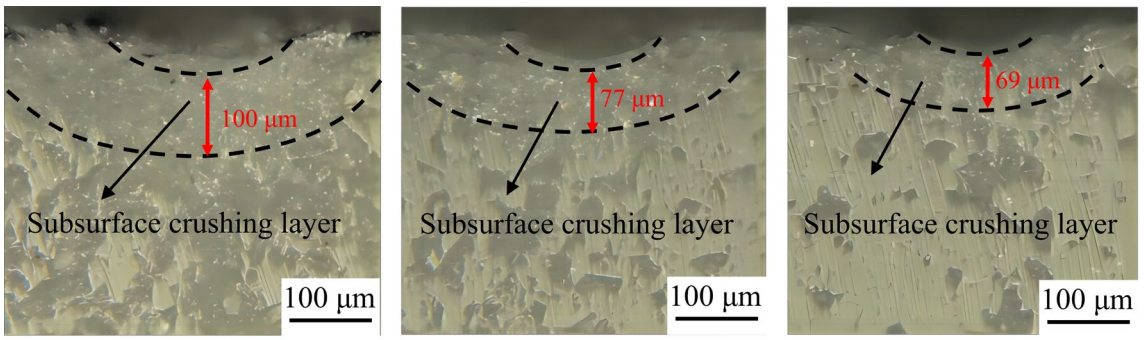

(a) 0 MPa (b) 200 MPa (c) 400 MPa

Fig. 7 Subsurface morphologies of scratches on 95% Al_2O_3 ceramic under different compressive pre-tresses

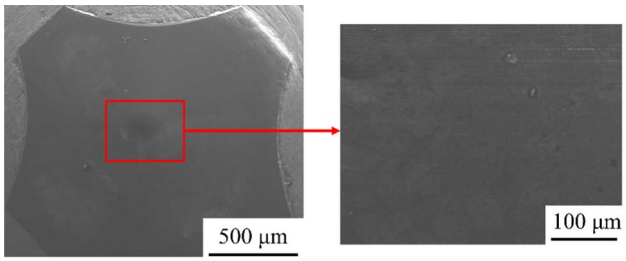

Fig. 8 Surface morphology of indenter under compressive pre-stress of 400 MPa at $t_1 = 20$ min

compressive pre-stress was increased to 400 MPa, there were some fine cracks at the tip of the indenter, and the area of wear at the tip of the indenter increased. Thus, it can be concluded that an increase in compressive pre-stress increases the wear of indenter.

3.3 Scratch Force

Figure 10 shows the variation trends of the tangential force F_y and normal force F_z of the diamond indenter during the 150-min scratch test. It was observed that as the scratch time increases, the normal and tangential forces of the scratch increase, and there is a linear relationship between the wear of the indenter and the change of Scratch force during the machining process. The Scratch force in the scratch process increases with an increase of compressive pre-stress, because compressive pre-stress changes the internal stress state of the alumina ceramic and suppresses the propagation process of internal cracks in the ceramic during the scratch process, as shown in Fig. 11. The fracture mode of the material changes from brittle to plastic, and the Scratch force mainly comes from the plastic deformation of the material, which continuously increases.

As shown in Fig. 12, the fluctuation of the scratch force ratio (F_y/F_z) decreases with the increase of compressive pre-stress, mainly because of the high brittleness of Al_2O_3 ceramics. During the contact extrusion process, the contact extrusion pressure between the indenter and the workpiece increases continuously. When the force reached the critical value of material fracture, the material broke, resulting in spalling, crushing, and grain pullout. After the material broke, the contact extrusion pressure between the indenter and the workpiece was released, eventually leading to fluctuations in the tangential force during the scratch process. During the scratch experiment, the Scratch force ratio was always greater than 2.0 at the compressive pre-stress of 400 MPa, which was 15% and 5% greater than the values at 0 MPa and 200 MPa respectively. This increases the difficulty of material processing. As the compressive pre-stress increases, the maximum tensile stress at the scratch decreases, indicating that the cracks formed during material processing decrease as the internal strength of the material increases, resulting in an increase in the scratch force ratio.

3.4 Vibration Signal

In the scratch process, the scratch force increases with the wear of the tool, so the difference in the scratch force can reflect the actual wear state of the tool, that is, the wear state of the tool determines the intensity of the vibration signal change. The variation of scratch force signal increases with the increase of tool wear. During normal use, tool wear is divided into three stages: initial wear, normal wear, and severe wear. In the indenter wear experiment, when the extrusion force is large, the workpiece is broken, thereby changing the vibration signal. Once the workpiece is damaged, the vibration signal is singular. The more severe the tool wear, the more drastic the change of the corresponding scratch force signal, and the singularity can reflect this severity. To better assess the wear state of the tool, wavelet transform [22] was used in this study to detect the singularity of the vibration signal during the scratch process. The collected signal was mainly the vibration generated by the contact between the tool and the workpiece, with the sampling frequency of 20 kHz and the sampling length of 600 points. The Daubechies (dbN) wavelet system is widely used in engineering applications. The Daubechies wavelet basis function was used with N = 8. The vibration signal was decomposed using six-layer wavelet. The vibration signal is shown in Fig. 13a, and the MATLAB wavelet decomposition results are shown in Fig. 13b–h. The acquired signals were preliminarily pre-processed, the low-frequency interference signal (a6) in the vibration signal was digitally filtered, and the filtered signal was decomposed into two layers of heuristic thresholds based on the wavelet threshold denoising method. The high-frequency noise component in the signal was removed, and a large number of noise information irrelevant to indenter wear was removed [27]. The low-frequency signal a6 of the sixth layer is the low-frequency signal component, and d1–d6 are the decomposed high-frequency signal components. The d_1 layer in Fig. 13h better identifies the location and distribution of signal singularities (peaks and troughs). Therefore, the analysis is performed on layer d1 in Fig. 13h.

The d1 layer wavelet decomposition results for the scratch force of the diamond indenters under different compressive pre-stresses at $t_1 = 10$ min and $t_2 = 120$ min are shown in Fig. 14 (intercept part of 0–100 collection points). When $t_1 = 10$ min, with the increase of compressive pre-stress, the distribution of singular points in the d1 layer signal and the corresponding maximum modulus (fluctuation value) gradually decrease; the contact vibration between the indenter and the workpiece decreases, because in the initial scratch stage, there are fewer cracks inside the ceramic. The compressive

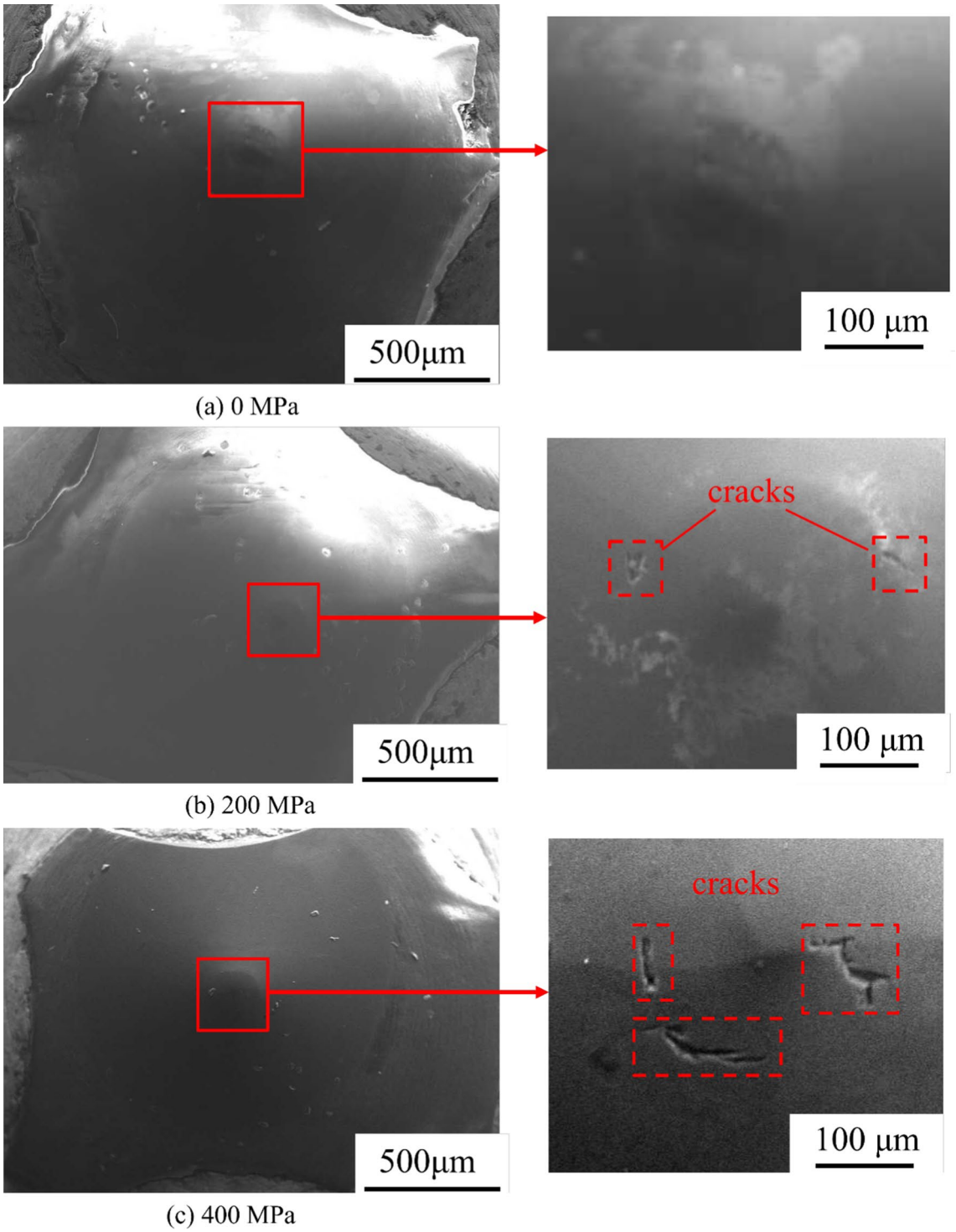

Fig. 9 Surface morphology of indenter after scratching for 150 min under different compressive pre-stresses: **a** 0 MPa; **b** 200 MPa; **c** 400 MPa

pre-stress improves the ceramic strength, making it closer. When $t_2 = 120$ min, the maximum modulus (fluctuation value) corresponding to the singular point distribution of the d1 layer obtained by wavelet decomposition of the scratch force of the indenters under different compressive pre-stresses is significantly increased compared with that at t_1. As the compressive pre-stress increases, the distribution of singular points in the d_1 layer signal and the corresponding maximum modulus (fluctuation value) gradually increase, and the vibration effect of the contact between

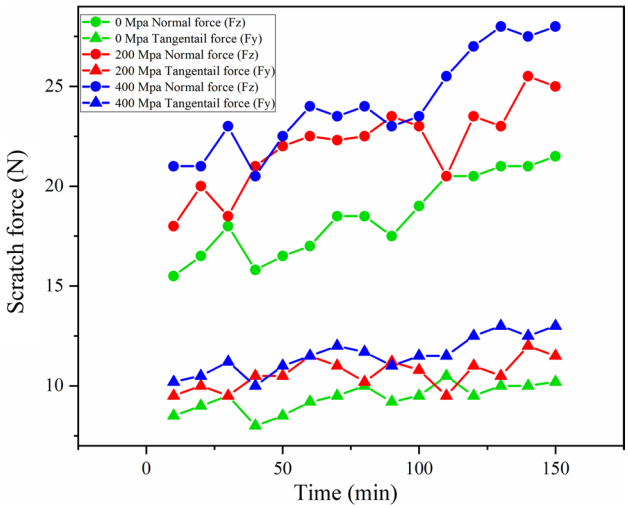

Fig. 10 Typical Scratch force–time curves under various compressive pre-stresses

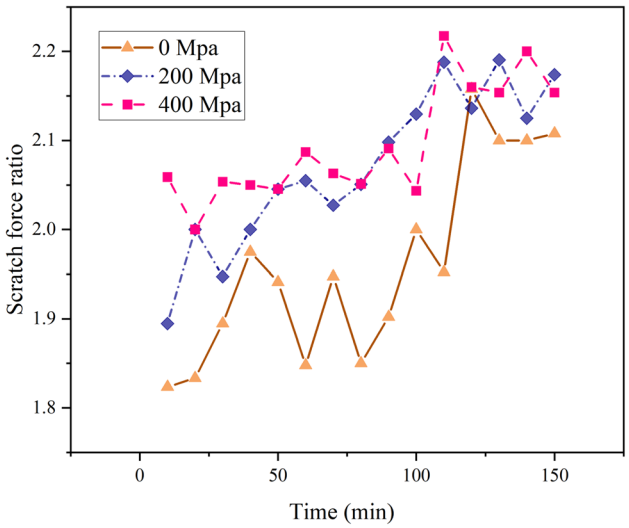

Fig. 12 Change in Scratch force ratio (tangential force/normal force) with time

the indenter and the workpiece gradually increases. When the compressive pre-stress is 400 MPa, the distribution of singular points and the corresponding maximum modulus (fluctuation value) in the d1 layer signal show an increasing trend compared with the compressive pre-stress of 0 MPa and 200 MPa.

After wavelet decomposition of the vibration signal, it is concluded that the signals in different frequency bands have certain energy. The vibration signals collected by the indenter at different wear stages were analyzed, and the changes in their energy as the scratch time increased in different frequency bands were analyzed.

During the scratch process, the main source of the vibration signal is the contact between the indenter and the workpiece.

According to previous studies [28–30], it is less affected by other interference using the signal energy feature extraction method. The db8 wavelet was used to decompose the collected signal into four wavelet packet layers. The sampling frequency was 20 kHz, the upper limit of the analysis frequency was fs/2, and the bandwidth of each frequency band was 10 kHz/24 = 625 Hz. The decomposed frequency bands were reconstructed to obtain the energy of each frequency band signal and the energy percentage distribution of each frequency band.

The energy characteristics of the vibration signal generated by the indenter during the scratching process were extracted and the energy percentage distribution of the indenter in each frequency band at different wear times was obtained, as shown in Fig. 15. It is observed that the vibration energy is mainly distributed in the first frequency band, and the energy in the first frequency band increases significantly with the increase of indenter wear.

The energy percentage in the first frequency band was determined under different compressive pre-stress scratches at different scratch times. In Fig. 16 shows the corresponding relationship between the energy percentage and the indenter wear process. During the initial wear stage of the indenter, the energy percentage in the first frequency band increases significantly. When the indenter

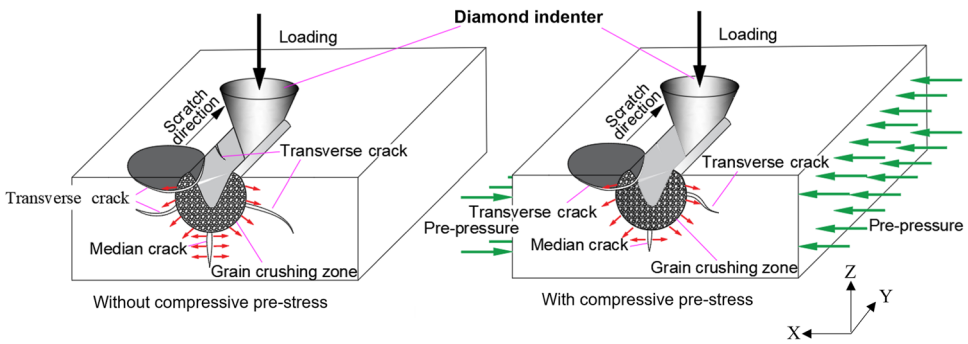

Fig. 11 Schematic of damage mechanisms during scratch

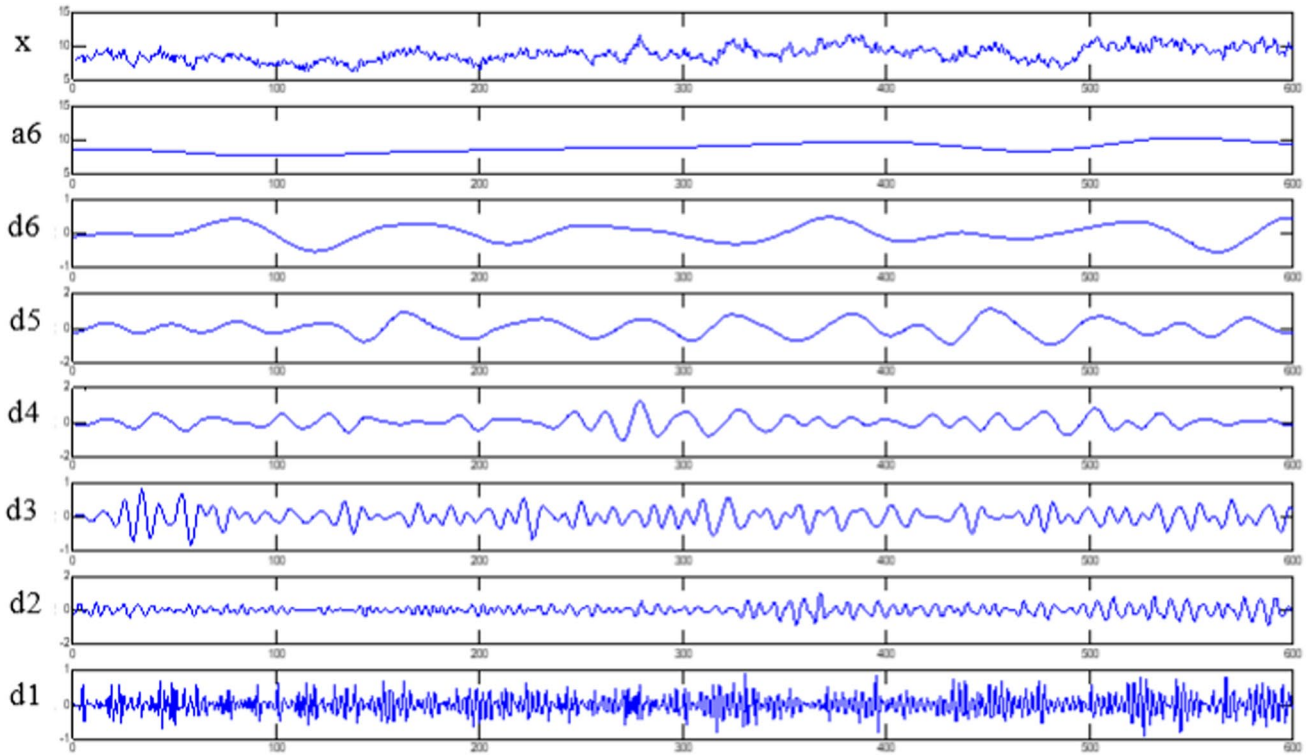

Fig. 13 Vibration signal and wavelet decomposition (x) and (a6): the low-frequency signal; (d1–d6): the high-frequency signal

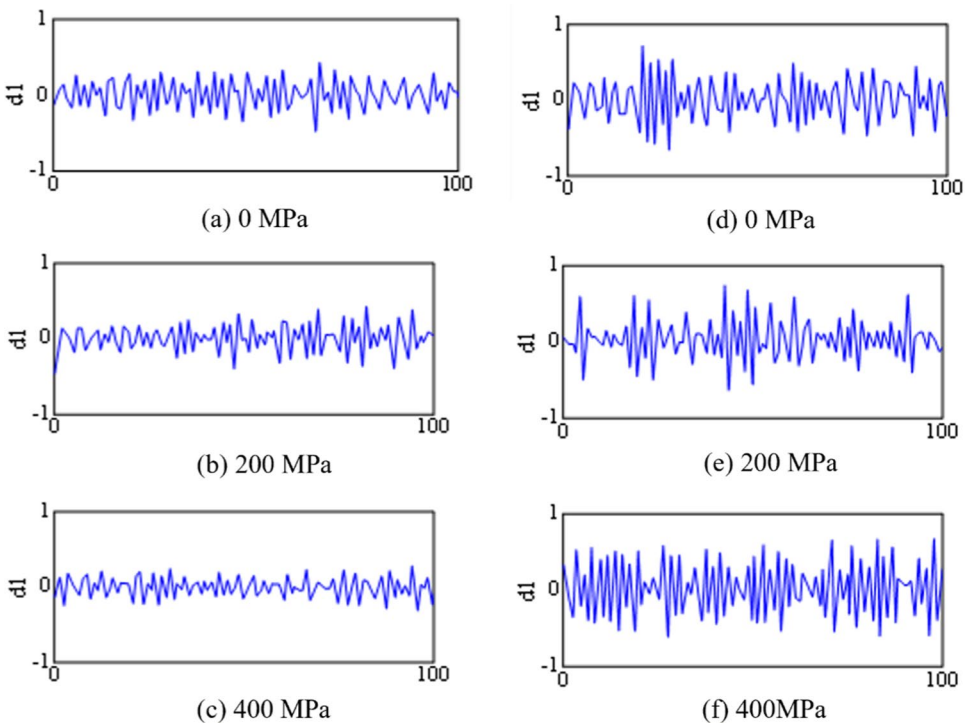

Fig. 14 Wavelet decomposition results for d1 layer at different scratch times and under different compressive prestresses. **a**–**c**: $t_1 = 10$ min; **d**–**f**: $t_2 = 120$ min

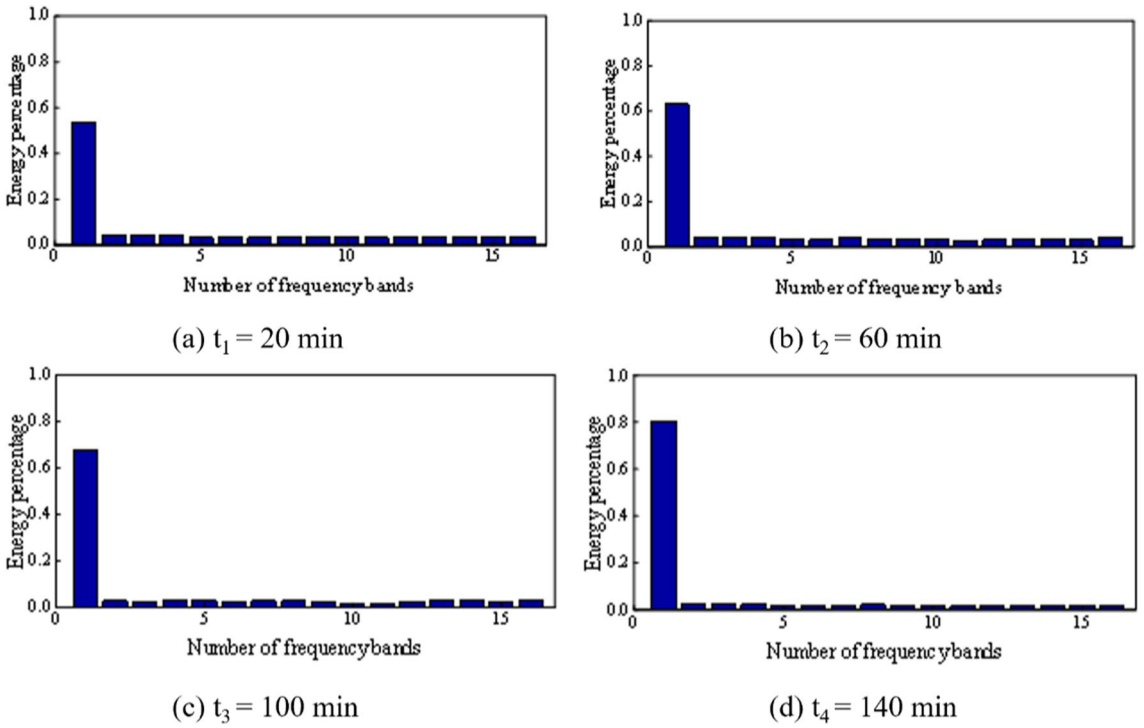

Fig. 15 Energy percentage of indenter at different scratch times (without compressive pre-stress)

Fig. 16 Energy percentage change in first frequency band of indenter with scratch time under different compressive pre-stresses

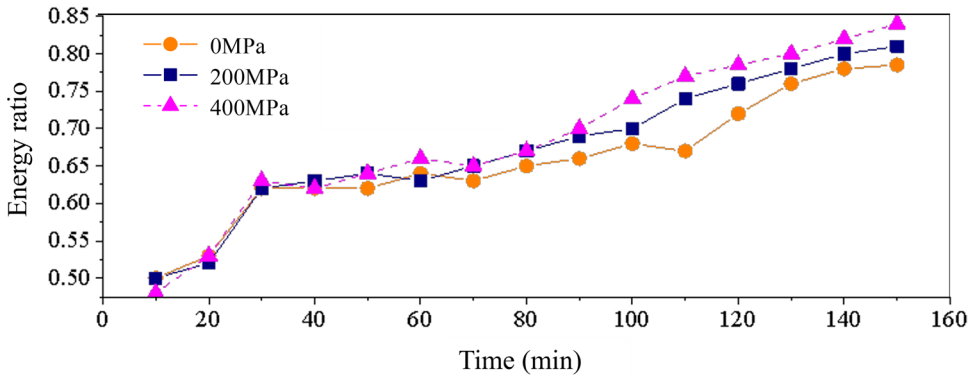

enters the normal wear stage, the energy percentage exhibits a stable increasing trend. As the indenter wear intensifies, the energy percentage increases (indenter wear increases slowly during ordinary scratch process). Further, when the scratch time exceeds 100 min, the energy percentage in the first frequency band increases with the increase of compressive pre-stress, which indirectly reflects that the degree of indenter wear under compressive pre-stress is greater than that of the indenter without compressive pre-stress, and increases with the increase of compressive pre-stress.

4 Conclusion

In this study, scratch experiments were conducted on 95% Al_2O_3 ceramics under different compressive pre-stresses using diamond indenters. The machining quality, indenter wear, as well as cutting force and vibration signal of the indenter were comprehensively analyzed. The main conclusions are as follows:

(1) With the increase of compressive pre-stress, the cracks and the groove width during the scratching process of 95% Al_2O_3 ceramic material can be gradually reduced. Although the indenter wear increases, but the scratch surface and subsurface damage can be effectively reduced, thereby achieving the purpose of good ceramic material removal rate and good processing quality. The compressive pre-stress helps to improve the flatness of the bottom and edge of the groove during the scratch process.

(2) With the increase of compressive pre-stress, the maximum tensile stress in the scratch area is reduced, and the cracks formed during the material processing decrease with the increase of internal strength, accompanied by the fluctuation of the cutting force during the scratching process is reduced.

(3) Combined with wavelet analysis, it is concluded that the energy percentage in the first frequency band corresponding to the indenter in the vibration signal increases with the increase of the compressive pre-stress, indicating that the wear of the indenter also gradually increases with the increase of the compressive pre-stress.

Funding This work was supported by the National Natural Science Foundation of China (Grant No. 52275406).

Declarations

Conflict of interest The authors declare no competing interests.

Ethical Approval Not applicable.

Consent to Participate Not applicable.

Consent to Publish All authors agree to publish.

References

1. Xie, J., Li, Q., Sun, J. X., & Li, Y. H. (2015). Study on ductile-mode mirror grinding of SiC ceramic freeform surface using an elliptical torus-shaped diamond wheel. *Journal of Materials Processing Technology, 222*, 422–433. https://doi.org/10.1016/j.jmatprotec.2015.03.027
2. Agarwal, S., & Rao, P. V. (2008). Experimental investigation of surface/subsurface damage formation and material removal mechanisms in SiC grinding. *International Journal of Machine Tools and Manufacture, 48*, 698–710. https://doi.org/10.1016/j.ijmachtools.2007.10.013
3. Lian, W., Liu, Y., Wang, W., Dong, Y., Wang, S., Liu, Z., & Liu, Y. (2022). Preparation of environmentally friendly low-cost mullite porous ceramics and the effect of waste glass powder on structure and mechanical properties. *International Journal of Precision Engineering and Manufacturing-Green Technology, 9*, 577–585. https://doi.org/10.1007/s40684-021-00333-8
4. Horvath, M., Kundrak, J., Mamalis, A. G., & Gyani, K. (2002). On the precision grinding of advanced ceramics. *The International Journal of Advanced Manufacturing Technology, 20*, 255–258. https://doi.org/10.1007/s001700200150
5. Malkin, S., & Hwang, T. W. (1996). Grinding mechanisms for ceramics. *CIRP Annals, 45*, 569–580. https://doi.org/10.1016/s0007-8506(07)60511-3
6. Zhang, B., Zheng, X. L., Tokura, H., & Yoshikawa, M. (2003). Grinding induced damage in ceramics. *Journal of Materials Processing Technology, 132*, 353–364. https://doi.org/10.1016/s0924-0136(02)00952-4
7. Lee, Y. J., & Wang, H. (2024). Sustainability of methods for augmented ultra-precision machining. *International Journal of Precision Engineering and Manufacturing-Green Technology, 11*, 585–624. https://doi.org/10.1007/s40684-023-00546-z
8. Feng, K., Zhao, L., Lyu, B., Xu, L., & Gu, Y. (2024). Study on the fabrication and grinding performance of the self-sharpening Cr_2O_3 Gel abrasive tool. *International Journal of Precision Engineering and Manufacturing, 25*, 713–729. https://doi.org/10.1007/s12541-024-00958-0
9. Chen, W., & Ravichandran, G. (1997). Dynamic compressive failure of a glass ceramic under lateral confinement. *Journal of the Mechanics and Physics of Solids, 45*, 1303–1328. https://doi.org/10.1016/s0022-5096(97)00006-9
10. Heard, H. C., & Cline, C. F. (1980). Mechanical behaviour of polycrystalline BeO, Al_2O_3 and AlN at high pressure. *Journal of Materials Science, 15*, 1889–1897. https://doi.org/10.1007/bf00550614
11. Yoshino, M., Aoki, T., & Shirakashi, T. (2001). Scratching test of hard-brittle materials under high hydrostatic pressure. *Journal of Manufacturing Science and Engineering, 123*, 231–239. https://doi.org/10.1115/1.1347035
12. Yoshino, M., Ogawa, Y., & Aravindan, S. (2005). Machining of hard-brittle materials by a single point tool under external hydrostatic pressure. *Journal of Manufacturing Science and Engineering, 127*, 837–845. https://doi.org/10.1115/1.2035695
13. Yoshino, M., Higashi, E., & Kawade, K. (2006). Development of a machining tester for two dimensional machining test under external hydrostatic pressure. *JSME International Journal Series C, 49*, 329–333. https://doi.org/10.1299/jsmec.49.329
14. Qu, S., Yao, P., Gong, Y., Yang, Y., Chu, D., & Zhu, Q. (2022). Modelling and grinding characteristics of unidirectional C-SiCs. *Ceramics International, 48*, 8314–8324. https://doi.org/10.1016/j.ceramint.2021.12.036
15. Yang, Y., Qu, S., & Gong, Y. (2021). Investigating the grinding performance of unidirectional and 2.5D-C/SiCs. *Ceramics International, 47*, 5123–5132. https://doi.org/10.1016/j.ceramint.2020.10.090
16. Tan, Y., Jiang, S., Yang, D., & Sheng, Y. (2011). Scratching of Al_2O_3 under pre-stressing. *Journal of Materials Processing Technology, 211*, 1217–1223. https://doi.org/10.1016/j.jmatprotec.2011.02.005
17. Tan, Y., Jiang, S., Nie, S., Yang, D., Zhang, G., & Peng, R. (2011). Prestress scratching on SiC ceramic. *International Journal of Applied Ceramic Technology, 9*, 322–328. https://doi.org/10.1111/j.1744-7402.2011.0202726.x
18. Zhang, G., Ma, W., Song, T., Du, C., Wang, Z., He, G., Xie, H., & Jiang, T. (2023). CA–MQL grinding of zirconia engineering ceramics under precompressive stress. *The International Journal of Advanced Manufacturing Technology, 126*, 5047–5056. https://doi.org/10.1007/s00170-023-11416-y
19. Du, C., Zhang, G., & Wang, H. (2021). Surface quality and residual stress variation of ceramics after abrasive grinding

under pre-compressive stress. *Ceramics International, 47*, 4315–4320. https://doi.org/10.1016/j.ceramint.2020.09.203
20. Uhlmann, E., & Spur, G. (1998). Surface formation in creep feed grinding of advanced ceramics with and without ultrasonic assistance. *CIRP Annals, 47*, 249–252. https://doi.org/10.1016/s0007-8506(07)62828-5
21. Glardon, R. E., & Finnie, I. (1981). Some observations on the wear of single point diamond tools used for machining glass. *Journal of Materials Science, 16*, 1776–1784. https://doi.org/10.1007/bf00540624
22. Yan, J., Syoji, K., & Tamaki, J. I. (2003). Some observations on the wear of diamond tools in ultra-precision cutting of single-crystal silicon. *Wear, 255*, 1380–1387. https://doi.org/10.1016/s0043-1648(03)00076-0
23. Goel, S., Luo, X., Reuben, R. L., & Pen, H. (2012). Influence of temperature and crystal orientation on tool wear during single point diamond turning of silicon. *Wear, 284–285*, 65–72. https://doi.org/10.1016/j.wear.2012.02.010
24. Peng, Y., Liang, Z., Wu, Y., Guo, Y., & Wang, C. (2011). Effect of vibration on surface and tool wear in ultrasonic vibration-assisted scratching of brittle materials. *The International Journal of Advanced Manufacturing Technology, 59*, 67–72. https://doi.org/10.1007/s00170-011-3473-5
25. Pastewka, L., Mrovec, M., Moseler, M., & Gumbsch, P. (2012). Bond order potentials for fracture, wear, and plasticity. *MRS Bulletin, 37*, 493–503. https://doi.org/10.1557/mrs.2012.94
26. Liu, T., Ma, L., Wang, Y., Bai, W., & Chang, H. (2019). Removal mechanism of machinable ceramics and theoretical model of cutting force in turning operation. *Mechanical Sciences, 10*, 429–436. https://doi.org/10.5194/ms-10-429-2019
27. Tran, M.-Q., Doan, H.-P., Vu, V. Q., & Vu, L. T. (2023). Machine learning and IoT-based approach for tool condition monitoring: A review and future prospects. *Measurement*. https://doi.org/10.1016/j.measurement.2022.112351
28. Kuo, C.-W., Shen, Y.-H., Yen, F.-L., Cheng, H.-Z., Hung, I. M., Wen, S.-B., Wang, M.-C., & Stack, M. (2014). Phase transformation behavior of 3mol% yttria partially-stabilized ZrO_2 (3Y–PSZ) precursor powder by an isothermal method. *Ceramics International, 40*, 3243–3251. https://doi.org/10.1016/j.ceramint.2013.09.112
29. Wang, C.-H., Wang, M.-C., Du, J.-K., Sie, Y.-Y., Hsi, C.-S., & Lee, H.-E. (2013). Phase transformation and nanocrystallite growth behavior of 2mol% yttria-partially stabilized zirconia (2Y-PSZ) powders. *Ceramics International, 39*, 5165–5174. https://doi.org/10.1016/j.ceramint.2012.12.013
30. Huang, H., & Liu, Y. C. (2003). Experimental investigations of machining characteristics and re-moval mechanisms of advanced ceramics in high speed deep grinding. *International Journal of Machine Tools and Manufacture, 43*, 811–823. https://doi.org/10.1016/s0890-6955(03)00050-6

Gaofeng Zhang is a professor at the School of Mechanical and Electrical Engineering of Changsha University. His main research areas include high-efficient and low-damage processing methods, tools and their engineering applications for difficult-to-machine materials.

Yu Liao is a master's degree jointly trained by Changsha University and Xiangtan University, is currently employed at Shenzhen Jinzhou Precision Technology Co., Ltd. Her main research direction is high-efficiency precision grinding, cutting and precision tool development.

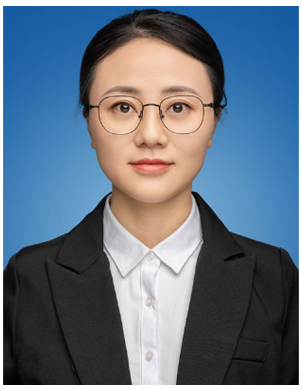

Yang Deng is a lecturer at the School of Mechanical and Electrical Engineering of Changsha University. Her research in recent years mainly involves the theory of high-efficiency and high-quality precision machining, and the development of high-speed machining coated tools.

Chang Liang is a lecturer at the School of Mechanical and Electrical Engineering of Changsha University, obtained his Ph.D. in Mechanical Engineering from Central South University in 2022. His primary research areas are precision grinding and laser micro-nano manufacturing.

Hang Xiao is a lecturer at the School of Mechanical and Electrical Engineering of Changsha University. He has extensive engineering experience in precision and ultra-precision manufacturing technologies for cutting and grinding equipment and processing technology.

Tiejun Song is a lecturer at the School of Mechanical Engineering and Mechanics, Xiangtan University, China. His current research interests include the design of complex tools, efficient processing of difficult-to-process materials, and non-destructive testing techniques.

Gang He obtained his Master's degree in Mechanical Engineering from Xiangtan University in 2023. His primary research focus is on efficient and precise grinding of difficult-to-machine materials.